



UDC 538.9

EDN ZZHQFC

<https://www.doi.org/10.33910/2687-153X-2025-6-1-9-16>

Charge transport mechanism and memristive effect in a thin film based on fluorinated polyaryl ether containing 1,4-dioxo-thioxanthene-9-one in-chain blocks

A. A. Gismatulin ¹, V. A. Pustovarov², D. S. Odintsov³, I. A. Os'kina³, I. K. Shundrina³, I. A. Azarov¹, L. A. Shundrin³, V. A. Gritsenko¹

¹ Rzhanov Institute of Semiconductor Physics, Siberian Branch of the Russian Academy of Sciences, 13 Lavrentiev Ave., Novosibirsk 630090, Russia

² Ural Federal University, 19 Mira Str., Ekaterinburg 620002, Russia

³ N. N. Vorozhtsov Institute of Organic Chemistry, Siberian Branch of the Russian Academy of Sciences, 9 Lavrentiev Ave., Novosibirsk 630090, Russia

Authors

Andrei A. Gismatulin, ORCID: [0000-0003-3177-6226](https://orcid.org/0000-0003-3177-6226), e-mail: aagismatulin@isp.nsc.ru

Vladimir A. Pustovarov, ORCID: [0000-0001-7373-1152](https://orcid.org/0000-0001-7373-1152), e-mail: v.a.pustovarov@urfu.ru

Danila S. Odintsov, ORCID: [0000-0002-6644-6211](https://orcid.org/0000-0002-6644-6211), e-mail: odintsov@nioch.nsc.ru

Irina A. Os'kina, ORCID: [0000-0001-5788-0182](https://orcid.org/0000-0001-5788-0182)

Inna K. Shundrina, ORCID: [0000-0003-1172-7523](https://orcid.org/0000-0003-1172-7523), e-mail: ishund@nioch.nsc.ru

Ivan A. Azarov, ORCID: [0000-0001-9571-2227](https://orcid.org/0000-0001-9571-2227), e-mail: azarov@isp.nsc.ru

Leonid A. Shundrin, ORCID: [0000-0002-5091-2812](https://orcid.org/0000-0002-5091-2812), e-mail: shundrin@nioch.nsc.ru

Vladimir A. Gritsenko, ORCID: [0000-0003-1646-0848](https://orcid.org/0000-0003-1646-0848), e-mail: grits@isp.nsc.ru

For citation: Gismatulin, A. A., Pustovarov, V. A., Odintsov, D. S., Os'kina, I. A., Shundrina, I. K., Azarov, I. A., Shundrin, L. A., Gritsenko, V. A. (2025) Charge transport mechanism and memristive effect in a thin film based on fluorinated polyaryl ether containing 1,4-dioxo-thioxanthene-9-one in-chain blocks. *Physics of Complex Systems*, 6 (1), 9–16. <https://www.doi.org/10.33910/2687-153X-2025-6-1-9-16> EDN ZZHQFC

Received 9 October 2024; reviewed 9 December 2024; accepted 9 December 2024.

Funding: The research related to the charge transport study was supported by the state contract under the ISP SB RAS program No. FWGW-2025-0010 The work on organic polymer synthesis as well as the fabrication of metal-polymer-silicon and memristor structures was funded by the state contract under the N. N. Vorozhtsov Institute of Organic Chemistry SB RAS program No. FWUE-2022-0007.

Copyright: © A. A. Gismatulin, V. A. Pustovarov, D. S. Odintsov, I. A. Os'kina, I. K. Shundrina, I. A. Azarov, L. A. Shundrin, V. A. Gritsenko (2025) Published by Herzen State Pedagogical University of Russia. Open access under CC BY-NC License 4.0.

Abstract. A new fluorinated thermally stable polyaryl ether with electron-withdrawing thioxanthene in-chain block (FPAE-ThS) was synthesized through the interaction of perfluorobiphenyl with 1,4-dihydroxy-9H-thioxanthene-9-one. The charge transport mechanism within the FPAE-ThS film is governed by the phonon-assisted tunneling between neighbouring traps. The thermal (1.0 eV) and optical trap (2.0 eV) ionization energies, as well as the trap concentration ($N = 1.0 \times 10^{20} \text{ cm}^{-3}$), are determined. The value of half Stokes shift (1.1 eV), obtained from the photoluminescence and photoluminescence excitation spectra, is consistent with the results of charge transport simulation. Furthermore, a prototype memory device based on the FPAE-ThS film demonstrates the resistive switching behavior with a four-order difference in the resistance between its low- and high-resistance states.

Keywords: fluorinated polymers, charge transport, memristor, trap, photoluminescence, photoluminescence excitation spectra

Introduction

The main advantages of organic devices over silicon-based counterparts include low cost of organic materials, inexpensive and environmentally friendly fabrication of organic electronic components using printing technologies and their versatile properties, such as lightweight, flexibility, transparency, durability, and reliability (Kronemeijer et al. 2014). Recently, a non-volatile memristor memory based on organic films has been developed (Shaposhnik et al. 2020; Yuan et al. 2021). This type of memory holds significant potential for next-generation flash memory and neuromorphic artificial intelligence devices.

The key requirements for organic polymers used in memristor technologies are their thermostability and ambipolarity. Specifically, the polymer structure must feature the alternating electron-donor and electron-acceptor chain blocks that facilitate the trap mechanism of electron transport. Thioxanthone (9*H*-thioxanthen-9-one) and its derivatives are electron acceptor compounds (Vasilieva et al. 2012) and found numerous practical applications (Jiang, Yin 2014a; 2014b; Kumar, Pereira 2020; Nazir et al. 2015; Neumann et al. 1997; Wang et al. 2014; Wang et al. 2018; Wu et al. 2014; Yilmaz et al. 2010). Recent studies have shown that the C-H fragments at the 1,4-positions of the 9*H*-thioxanthen-9-one ring can be replaced by OH groups during the cyclization of arylsulfanylbenzoic acid and benzoquinone (Loskutov, Beregovaya 2009), yielding the corresponding 1,4-dihydroxy-1*H*-thioxanthen-9-one (**1**, Fig. 1). Compound **1** was found to be a strong electron acceptor (Odintsov et al. 2023). The presence of two functional OH groups in the structure of compound **1** provides an opportunity to synthesize an electroactive polymer containing thioxanthone-like structures as an effective electron-acceptor in-chain block. This motivated us to synthesize fluorinated polyaryl ether with electron acceptor 1,4-dioxy-9*H*-thioxanthen-9-one in-chain blocks (FPAE-ThS, Fig. 1) for its potential application in polymer-based resistive memory devices. Notably, polyfluoroaromatic fragments were not previously used in the design of electroactive polymers for this purpose. Perfluorobiphenyl was chosen as the second monomer for polycondensation because of its regioselective reactivity with nucleophiles, which is facilitated by the reactive F atoms at the 1,8-positions of the cycle. Meanwhile, the presence of two F atoms in the ortho-positions of the benzene rings may also reduce the π -conjugation between the thioxanthone and tetrafluorophenyl fragments of the polymer chain, thus, increasing the polymer energy gap (E_g), and preventing the emergence of semiconducting properties.

The study of charge transport mechanisms, in particular leakage currents, can provide insights into the trap nature of polymer films through the characterization of trap energies (Gismatulin et al. 2024). Time-of-flight transient experiments on polymers showed that the logarithm mobility is proportional to the square root of the electric field (\sqrt{F}) (Dunlap et al. 1996; Hirao et al. 1995; Novikov et al. 1998). This dependence is formally described by the Frenkel law in inorganic dielectric films (Frenkel 1938; Ganichev et al. 2000; Gritsenko et al. 2018; Schroeder 2015).

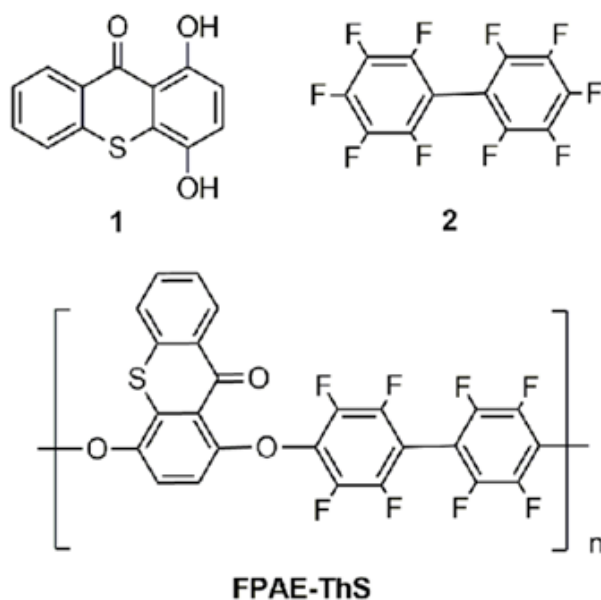


Fig. 1. Structures of 1,4-dihydroxy-1*H*-thioxanthen-9-one (**1**), perfluorobiphenyl (**2**) and FPAE-ThS

The primary objective of the reported study is to explore the charge transport mechanisms within thin FPAE-ThS films and to determine the trap parameters that govern the charge transport. In addition, the potential of using FPAE-ThS films as an active medium in memristor devices was investigated.

Methods

FPAE-ThS was synthesized through the nucleophilic polycondensation of monomers **1** and **2** in dimethylacetamide using K_2CO_3 to increase the basicity of the solution (ESI). FPAE-ThS showed good molecular weight properties for forming thin films on Si wafers and demonstrated its thermal stability up to 247 °C. Its electrochemical reduction/oxidation activity confirmed the ability of FPAE-ThS to facilitate the charge transport (ESI). The polymer has an energy gap (E_g) of 3.02 eV, which classifies FPAE-ThS as a dielectric material (ESI).

To investigate the trap ionization mechanism in the FPAE-ThS film, experimental current density (j) and electric field (F) characteristics, measured at different temperatures, were compared with different theoretical models (Gismatulin et al. 2024).

To fabricate metal-insulator-silicon (MIS) structures, FPAE-ThS polymer films were deposited from a 1% FPAE-ThS solution in chloroform on Si (100) p-type silicon substrates, with the resistances of 10 Ohm×cm and 0.001 Ohm×cm, by spin coating using the SpinNXG-P1AC spin coater. Prior to deposition, the Si substrate was treated with a 10% HF solution to remove the native oxide layer. An array of upper aluminum (Al) electrodes was sputtered onto the FPAE-ThS layer through a shadow mask by thermal sputtering, with a contact area of 0.5 mm². To enhance the electrical contact for j - F measurements, the bottom electrode was also thermally sputtered over the entire area of the non-planar Si substrate. The j - F characteristics of the Si/FPAE-ThS/Al structure were measured using a Keithley 2400 electrometer. Measurements were conducted over a temperature range of 300 to 375K using a Linkam LTS420E cell, with the temperature controlled by a Linkam T95 temperature controller. The voltage ramp rate was set to 0.9 V/sec.

The thickness and refractive index of the FPAE-ThS films were measured using an Ellips-1881 SAG spectral ellipsometer. A film thickness of 110 nm was used to study the charge transport mechanism, while a film thickness of 25 nm was employed for the memristor structure.

The photoluminescence (PL) spectra in the range of 1.7–3.3 eV and the photoluminescence excitation (PLE) spectra in the range of 3.3–5.2 eV were measured at the temperature of 4.4 K. Measurements were carried out using a HORIBA iXR320 FLUOROLOG spectrometer, equipped with a cooled Synapse plus CCD camera (Horiba) as a detector and a 150 W ozone-free Xe lamp. A closed-cycle cryogenic system and a high-vacuum helium cryostat (Trade Engineering, Russia) with an RDK-205D2 cryohead (Japan), controlled by a Lake Shore 331 temperature controller, were used to cool the sample. The PL spectra were recorded with a spectral resolution of 2 nm, while the PLE spectra were normalized to the number of exciting photons using a calibrated photodiode. The PL spectra are presented without normalization to the spectral sensitivity of the detection system.

The transverse charge transport mechanism in a copolymer is similar to that in a dielectric due to its high energy gap. It is described by the following expression (Gismatulin et al. 2024; Gritsenko et al. 2018):

$$j = \frac{e}{a^2} P = eN^{\frac{2}{3}} P, \quad (1)$$

where j is the current density, e is the electron charge, a is the average distance between traps, $N = a^{-3}$ is the trap concentration, and P is the trap ionization probability.

The exponential dependence of the current density on the electric field in the Frenkel effect arises from the reduction in the Coulomb barrier under the influence of the electric field. The trap ionization probability in the Frenkel model is described by the following expression (Frenkel 1938):

$$P = \nu \exp \left(- \frac{W - \left(\frac{e^3}{\pi \epsilon_{\infty} \epsilon_0} \right)^{\frac{1}{2}} \sqrt{F}}{kT} \right), \quad (2)$$

where $\nu = W/h$ is the attempt to escape factor, W is the trap ionization energy, h is the Planck constant, $\epsilon_{\infty} = n^2$ is the high-frequency permittivity, n is the refractive index, ϵ_0 is the dielectric constant, F is the electric field, k is the Boltzmann constant, and T is the temperature.

For high concentrations of neutral traps, the phonon-assisted tunneling mechanism between neighboring traps, as proposed by Nasyrov and Gritsenko, is applicable. In this model, electron tunneling occurs from one trap to a neighboring trap, rather than ionization into the FPAE-ThS conduction band, due to the short distance between traps (Odintsov et al. 2022).

The trap ionization probability in the Nasyrov and Gritsenko phonon-assisted tunneling model between neighboring traps is given by the expression (Nasyrov, Gritsenko 2011):

$$P = \frac{2\sqrt{\pi}\hbar W_t}{m^* a^2 \sqrt{2kT(W_{opt} - W_t)}} \exp\left(-\frac{W_{opt} - W_t}{kT}\right) \exp\left(-\frac{2a\sqrt{2m^* W_t}}{\hbar}\right) \sinh\left(\frac{eFa}{2kT}\right), \quad (3)$$

where, \hbar is the reduced Planck constant, W_t is the thermal trap ionization energy, m^* is the effective mass, and W_{opt} is the optical trap ionization energy.

Results and discussion

The refractive index (n) and absorption coefficient (α) are shown in Fig. 2. These optical constants were determined by reconstructing the data from multiple angles using an inverse ellipsometry approach, applying optimization techniques for each photon energy individually. In the ultraviolet region, three distinct peaks are observed in both the refractive index and the absorption coefficient, corresponding to photon energies of 3.1 eV, 3.9 eV and 4.5 eV. The refractive index in the infrared region is consistent with values typically found in similar organic films (Odintsov et al. 2022). At a photon energy of 1.1 eV, the refractive index of the FPAE-ThS film is measured to be 1.49, as shown in Fig. 2.

The experimental j - F characteristics of the p-Si/FPAE-ThS/Al structure were simulated by the Frenkel model (see Fig. 3(a)). The corresponding trap ionization energy (W) obtained from the simulation is 0.55 eV. The attempt-to-escape factor (ν) was then calculated using the Einstein relation: $\nu = W/h$, giving a value of $1.3 \times 10^{14} \text{ sec}^{-1}$ at the trap ionization value of 0.55 eV. The high-frequency dielectric constant parameter value obtained from the simulation is 19. Alternatively, the high-frequency dielectric constant can be derived from the expression $\epsilon_\infty = n^2 = (1.49)^2 = 2.22$. Thus, the Frenkel effect is not a suitable model to describe the charge transport and trap ionization in the FPAE-ThS film. In addition, the Frenkel model predicts an extraordinarily low trap concentration value, $N = 1.5 \times 10^{11} \text{ cm}^{-3}$, which is inconsistent with typical trap concentrations in inorganic dielectrics, normally ranging from 10^{18} to 10^{21} cm^{-3} (Nasyrov, Gritsenko 2013).

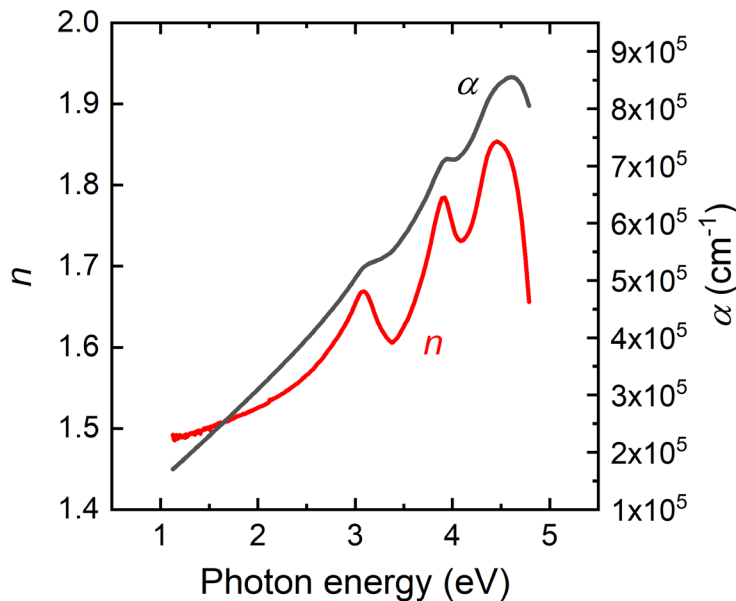


Fig. 2. Refractive index (n) and absorption coefficient (α) of the FPAE-ThS film at different quantum energies

In the Nasyrov and Gritsenko model, the trap ionization probability exhibits an exponential dependence on the intertrap distance, $a = N^{-1/3}$, or, equivalently, on the trap concentration N . Thus, the trap concentration can be determined from the curve slope of the j - F characteristic (see Fig. 3(b)). The simulation results based on the Nasyrov and Gritsenko model give the following fitting parameters: trap concentration $N = 1.0 \times 10^{20} \text{ cm}^{-3}$, thermal trap ionization energy $W_t = 1.0 \text{ eV}$, optical trap ionization energy $W_{\text{opt}} = 2.0 \text{ eV}$ and effective electron mass $m^* = 0.39 m_e$.

The PL spectra of the FPAE-ThS film are shown in Fig. 4. A broad peak in the range of 2.25–2.45 eV predominates the PL spectrum. In addition, the PLE spectrum, shown in Fig. 5, reveals three maxima at 3.80, 4.55 and 5.05 eV. Notably, the PLE peaks at 3.8 eV and 4.55 eV coincide with the peaks in the refractive index and absorption coefficient spectra of the FPAE-ThS film, suggesting that the luminescence centers of the FPAE-ThS film are associated with these energy levels. The thermal trap energy $W_t = 1.0 \pm 0.1 \text{ eV}$ obtained from the charge transport simulation is in agreement with the half Stokes shift value of $1.1 \pm 0.1 \text{ eV}$ of the PL and PLE spectra.

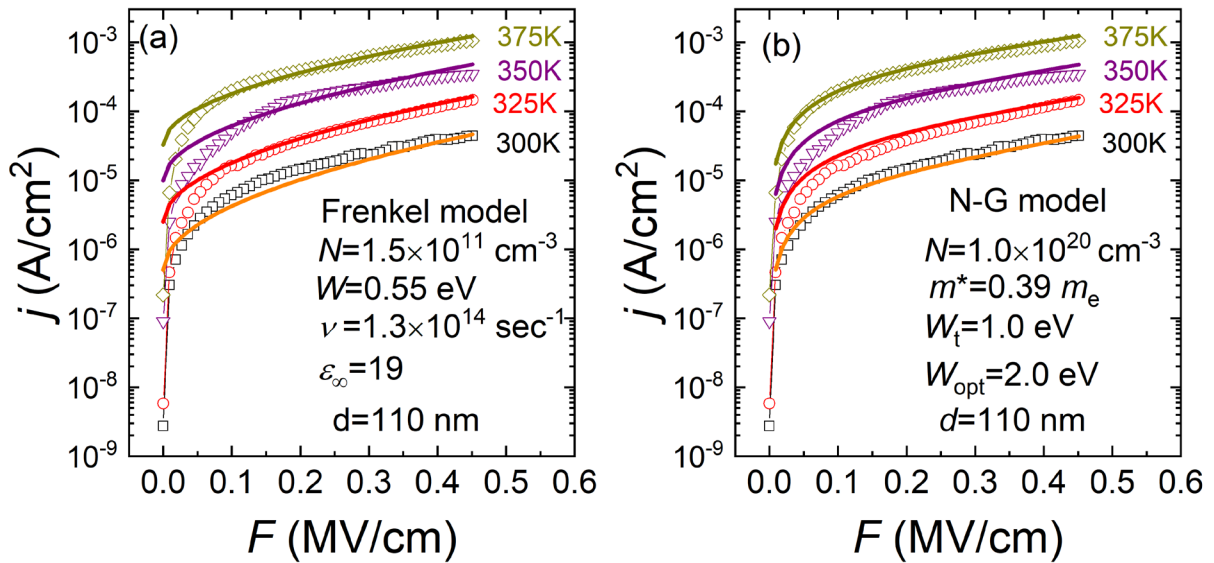


Fig. 3. j - F characteristics of the FPAE-ThS-based structure at various temperatures, along with simulations using (a) the Frenkel model and (b) the Nasyrov-Gritsenko model

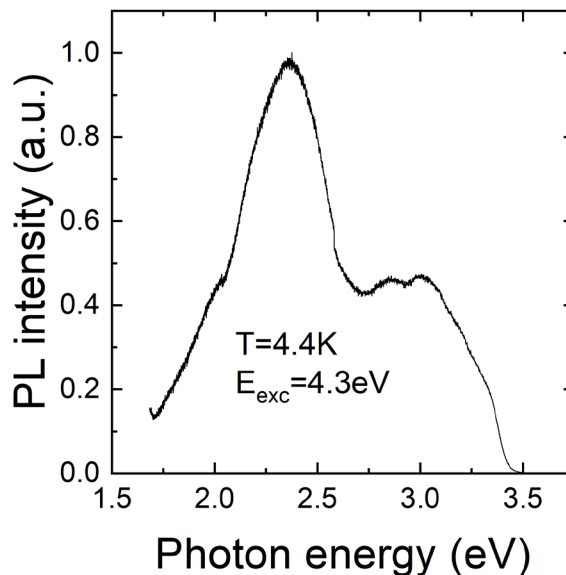


Fig. 4. Photoluminescence spectra of the FPAE-ThS film at a temperature of 4.4 K

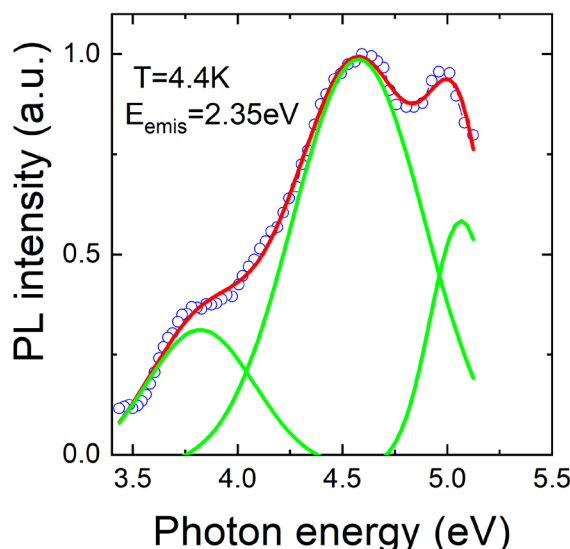


Fig. 5. Photoluminescence excitation spectrum (2.35 eV emission band) of the FPAE-ThS film at a temperature of 4.4 K (blue circles). The green curves represent the decomposition of the spectrum into three peaks, the red line denotes the sum of these individual components

The potential application of the FPAE-ThS film as an active medium in a memristor is demonstrated through the p^{++} -Si/FPAE-ThS/Al MIS structure (see Fig. 6). This structure, with a 25 nm thick FPAE-ThS film, shows its reversible resistive switching behavior from the high resistance state (HRS) to the low resistance state (LRS) when the voltage sweep is increased from 0 V to +3V and from the LRS to the HRS when the voltage sweep is reversed from 0 V to -2.5V. (Fig. 6). The FPAE-ThS-based memristor is a low-power memory device, making it a promising candidate for practical applications in the Resistive Random-Access Memory (ReRAM) technology, which requires switching voltages of less than 5 V.

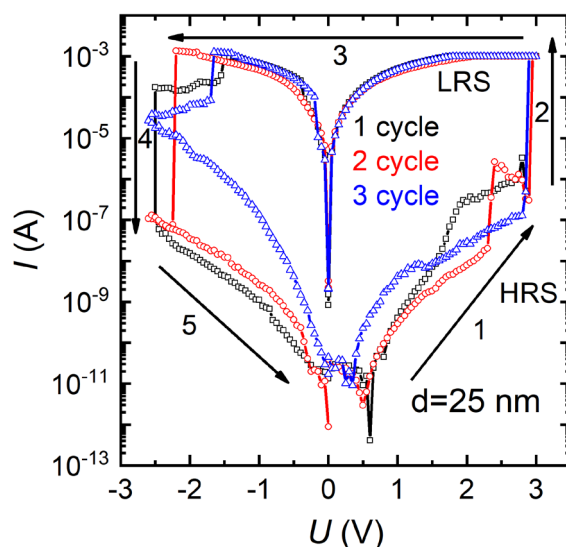


Fig. 6. current-voltage characteristics of the FPAE-ThS-based memristor, with arrow numbers 1 to 5 indicating the voltage sweep direction

Conclusions

We described the synthesis and properties of a novel electroactive polyaryl ether containing an electron-withdrawing thioxanthone in-chain block and a polyfluoroaromatic tetrafluorobiphenyl fragment. This fragment was used for the first time in the design of organic polymers for practical applications

in memristor technologies. The charge transport mechanism in the thin FPAE-ThS film was studied by measuring the current density-electric field characteristics of the corresponding MIS structures at different temperatures and modelling the experimental data using both the Frenkel model and the Nasyrov-Gritsenko model of phonon-assisted tunneling between traps. It was shown that the Frenkel model fails to describe the experimental data, predicting an anomalously high value of the high-frequency permittivity and an anomalously low trap concentration. In contrast, the Nasyrov-Gritsenko model of phonon-assisted tunneling between traps quantitatively describes the experimental data, yielding values for the thermal ($W_t = 1.0$ eV) and optical ($W_{opt} = 2.0$ eV) trap energies, as well as a reasonable trap concentration ($N = 1.0 \times 10^{20}$ cm⁻³) for the FPAE-ThS film. These results indicate that the charge transport in the FPAE-ThS film is effectively described by a multiphonon mechanism, similar to processes occurring in semiconductors and inorganic dielectrics. Moreover, the thermal trap energy derived from the simulation of the charge transport mechanism in FPAE-ThS films is consistent with the half Stokes shift value observed in the PL and PLE spectra of the FPAE-ThS film, taking into account measurement and simulation errors. In addition, FPAE-ThS was shown to be a viable active layer for memristors. The FPAE-ThS-based memristor structure has low switching voltages and a 4-order resistance ratio between HRS and LRS, thus making it particularly advantageous for applications in the Resistive Random-Access Memory (ReRAM) technology.

Conflict of Interest

The authors declare that there is no conflict of interest, either existing or potential.

Author Contributions

All authors contributed equally to the final work, engaging in discussions and collaborating on the writing of the article.

Acknowledgements

The authors acknowledge the Core Facilities VTAN NSU and the Multi-Access Chemical Research Center of the Siberian Branch of the Russian Academy of Sciences for granting an access to their experimental equipment and instrumental facilities.

References

- Dunlap, D. H., Parris, P. E., Kenkre, V. M. (1996) Charge-dipole model for the universal field dependence of mobilities in molecularly doped polymers. *Physical Review Letters*, 77, article 542. <https://doi.org/10.1103/PhysRevLett.77.542> (In English)
- Frenkel, J. (1938) On pre-breakdown phenomena in insulators and electronic semi-conductors. *Physical Review*, 54, 647–648. <https://doi.org/10.1103/PhysRev.54.647> (In English)
- Ganichev, S. D., Ziemann, E., Prettl, W. et al. (2000) Distinction between the Poole-Frenkel and tunneling models of electric-field-stimulated carrier emission from deep levels in semiconductors. *Physical Review B*, 61, 10361–10365. <https://doi.org/10.1103/PhysRevB.61.10361> (In English)
- Gismatulin, A. A., Odintsov, D. S., Shundrina, I. K. et al. (2024) Charge transport mechanism and trap origin in methyl methacrylate copolymer with thioxanthone side groups. *Chemical Physics Letters*, 840, article 141140. <https://doi.org/10.1016/j.cplett.2024.141140> (In English)
- Gritsenko, V. A., Perevalov, T. V., Voronkovskii, V. A. et al. (2018) Charge transport and the nature of traps in oxygen deficient tantalum oxide. *ACS Applied Materials & Interfaces*, 10, 3769–3775. <https://doi.org/10.1021/acsami.7b16753> (In English)
- Hirao, A., Nishizawa, H., Sugiuchi, M. (1995) Diffusion and drift of charge carriers in molecularly doped polymers. *Physical Review Letters*, 75, 1787–1790. <https://doi.org/10.1103/PhysRevLett.75.1787> (In English)
- Jiang, X., Yin, J. (2014a) Copolymeric photoinitiators containing in-chain thioxanthone and coinitiator amine for photopolymerization. *Journal of Applied Polymer Science*, 94, 2395–2400. <https://doi.org/10.1002/app.21178> (In English)
- Jiang, X., Yin, J. (2014b) Polymeric photoinitiator containing in-chain thioxanthone and coinitiator amines. *Macromolecular Rapid Communications*, 25, 748–752. <https://doi.org/10.1002/marc.200300270> (In English)
- Kronemeijer, A. J., Pecunia, V., Venkateshvaran, D. et al. (2014) Two-dimensional carrier distribution in top-gate polymer field-effect transistors: correlation between width of density of localized states and Urbach energy. *Advanced Materials*, 26, 728–733. <https://doi.org/10.1002/adma.201303060> (In English)

- Kumar, M., Pereira, L. (2020) Towards highly efficient TADF yellow-red OLEDs fabricated by solution deposition methods: Critical influence of the active layer morphology. *Nanomaterials*, 10 (1), article 101. <https://doi.org/10.3390/nano10010101> (In English)
- Loskutov, V. A., Beregovaya, I. V. (2009) Reaction of thiosalicylic acid with 1,4-quinones and cyclization of the resulting arylsulfanylbenzoic acids. *Russian Journal of Organic Chemistry*, 45, 1405–1409. <https://doi.org/10.1134/S1070428009090152> (In English)
- Nasyrov, K. A., Gritsenko, V. A. (2011) Charge transport in dielectrics via tunneling between traps. *Journal of Applied Physics*, 109, article 093705. <https://doi.org/10.1063/1.3587452> (In English)
- Nasyrov, K. A., Gritsenko, V. A. (2013) Transport mechanisms of electrons and holes in dielectric films. *Physics Uspekhi*, 56, 999–1012. <https://doi.org/10.3367/UFNe.0183.201310h.1099> (In English)
- Nazir, R., Balciunas, E., Buczynska, D. et al. (2015) Donor–acceptor type thioxanthenes: Synthesis, optical properties, and two-photon induced polymerization. *Macromolecules*, 48, 2466–2472. <https://doi.org/10.1021/acs.macromol.5b00336> (In English)
- Neumann, M. G., Gehlen, M. H., Encinas, M. V. et al. (1997) Photophysics and photoreactivity of substituted thioxanthenes. *Journal of the Chemical Society, Faraday Transactions*, 93, 1517–1521. <https://doi.org/10.1039/A607264J> (In English)
- Novikov, S. V., Dunlap, D. H., Kenkre, V. M. et al. (1998) Essential role of correlations in governing charge transport in disordered organic materials. *Physical Review Letters*, 81, article 4472. <https://doi.org/10.1103/PhysRevLett.81.4472> (In English)
- Odintsov, D. S., Shundrina, I. K., Gismatulin, A. A. et al. (2022) Heat-resistant polyimides with electron-acceptor pendant groups of the thioxanthenone series for resistive storage devices with a low switching voltage. *Journal of Structural Chemistry*, 63, 1811–1819. <https://doi.org/10.1134/S0022476622110117> (In English)
- Odintsov, D. S., Os'kina, I. A., Irtegovaya, I. G. et al. (2023) Electrochemical reduction of 1*H*-thioxanthene-1,4,9-trione and 3-methyl-1*H*-thioxanthene-1,4,9-trione—representatives of a new class of heterocycles related to thioxanthenone. *European Journal of Organic Chemistry*, 26 (33), article e202300459. <https://doi.org/10.1002/ejoc.202300459> (In English)
- Schroeder, H. (2015) Poole-Frenkel-effect as dominating current mechanism in thin oxide films — an illusion?! *Journal of Applied Physics*, 117, article 215103. <https://doi.org/10.1063/1.4921949> (In English)
- Shaposhnik, P. A., Zapunidi, S. A., Shestakov, M. V. et al. (2020) Modern bio and chemical sensors and neuromorphic devices based on organic semiconductors. *Russian Chemical Reviews*, 89, 1483–1506. <https://doi.org/10.1070/rcr4973> (In English)
- Vasilieva, N. V., Irtegovaya, I. G., Loskutov, V. A. et al. (2012) Redox properties and radical anions of 2-substituted thioxanthen-9-ones and their 2-methyl *S*-oxide derivatives. *Mendeleev Communications*, 23 (6), 334–336. <https://doi.org/10.1016/j.mencom.2013.11.010> (In English)
- Wang, H., Xie, L., Peng, Q. et al. (2014) Novel thermally activated delayed fluorescence materials—thioxanthenone derivatives and their applications for highly efficient OLEDs. *Advanced Materials*, 26, 5198–5204. <https://doi.org/10.1002/adma.201401393> (In English)
- Wang, Y., Zhu, Y., Xie, G. et al. (2018) Red thermally activated delayed fluorescence polymers containing 9*H*-thioxanthen-9-one-10,10-dioxide acceptor group as pendant or incorporated in backbone. *Organic Electronics*, 59, 406–413. <https://doi.org/10.1016/j.orgel.2018.05.058> (In English)
- Wu, Q., Xiong, Y., Liang, Q. et al. (2014) Developing thioxanthenone based visible photoinitiators for radical polymerization. *RSC Advances*, 4, article 52324. <https://doi.org/10.1039/C4RA07614A> (In English)
- Yilmaz, G., Tuzun, A., Yaggi, Y. (2010) Thioxanthenone–carbazole as a visible light photoinitiator for free radical polymerization. *Journal of Polymer Science. Part A: Polymer Chemistry*, 48, 5120–5125. <https://doi.org/10.1002/pola.24310> (In English)
- Yuan, L., Liu, S., Chen, W. et al. (2021) Organic memory and memristors: From mechanisms, materials to devices. *Advanced Electronic Materials*, 7 (11), article 2100432. <https://doi.org/10.1002/aelm.202100432> (In English)